2020년 8월
석사학위 논문

Synthesis, characterization and biological evaluation of *N*-substituted asymmetric squaraines for photodynamic therapy

조 선 대 학 교 대 학 원

화 학 과

최 형 진

Synthesis, characterization and biological evaluation of *N*-substituted asymmetric squaraines for photodynamic therapy

광역학 치료를 위한 N-치환된 비대칭성 스쿠아레인 화합물의 합성, 분석 및 생물학적 평가

2020년 8월 28일

조 선 대 학 교 대 학 원

화 학 과

최 형 진

Synthesis, characterization and biological evaluation of *N*-substituted asymmetric squaraines for photodynamic therapy

지도교수 이 종 대

이 논문을 이학석사학위신청 논문으로 제출함.

2020년 5월

조 선 대 학 교 대 학 원

화 학 과

최 형 진

최형진의 석사학위논문을 인준함

위원장 조선대학교 교수 손 홍 래 (인)

위 원 조선대학교 교수 김 호 중 (인)

위 원 조선대학교 교수 이 종 대 (인)

2020년 6월

조 선 대 학 교 대 학 원

TABLE OF CONTENTS

Synthesis, characterization and biological evaluation of *N*-substituted asymmetric squaraines for photodynamic therapy

LIST OF FIGURES

LIST OF SCHEME

Abstract

Synthesis, characterization and biological evaluation of N-substituted asymmetric squaraines for photodynamic therapy

Hyung Jin Choi
Advisor : Prof. Lee Jong Dae, Ph.D,
Department of Chemistry,
Graduate School of Chosun University

Photodynamic therapy (PDT) is a clinically established and highly evolving treatment modality for cancer. PDT utilizes a light responsive drug called photosensitizer that selectively destroys tumor cells upon light irradiation. Squaraine dyes are a class of organic dyes with strong and narrow absorption bands in the near-infrared. Despite high molar absorptivities and fluorescence quantum yields, these dyes have been less explored than other dye scaffolds due to their susceptibility to nucleophilic attack. Recent strategies in probe design including encapsulation, conjugation to biomolecules, and new synthetic modifications have seen squaraine dyes emerging into the forefront of biomedical imaging and other applications. In addition, squaraines are a class of dyes possessing all favorable characteristics of a photosensitizer and have been considered to be a potent candidate for next generation PDT. In this study we chose an N-alkylated asymmetric derivatives of squaraine which has been reported for its tumor specificity but least studied for its cellular and molecular functions. Our studies revealed that the N-alkylated asymmetric derivatives of squaraine possess maximum photodynamic activity in human colon cancer cells HCT116 and had very little cytotoxicity in normal colon cells Ccd-18co. We analyzed its pro and anti-apoptotic events initiated by oxidative stress exploring a proteomic approach and delineated other critical molecular pathways and key proteins involved in regulating the

complex network of cellular response upon PDT. Our study showed that, N-alkylated asymmetric squaraines predominantly accumulate in mitochondria and induce mitochondriamediated apoptosis. Our study also reveals the novel mechanistic role of N-alkylated asymmetric squaraines to induce oxidative stress there by activating both protective and death inducing pathways post PDT.

초록

광역학 치료를 위한 N-치환된 비대칭성 스쿠아레인 화합물의 합성, 분석 및 생물학적 평가

석사과정 : 최 형 진
지도교수 : 이 종 대
조선대학교 화학과

광역학 치료(PDT)는 임상적으로 확립되어 있고 고도로 발전한 암 치료법입니다. PDT는 광 조사시 종양세포를 선택적으로 파괴하는 감광제(photoensitizer)라는 광 반응성 약물을 사용합니다. Squaraine 화합물은 근적외선 내에서 강하고 좁은 흡수 띠를 가지는 유기 염료의 일종입니다. 캡슐화, 생체 분자 결합, 새로운 합성 수정 등 최근 Squaraine 화합물이 생체 의학 imaging 및 기타 응용 분야에서 중심으로 부상하고 있습니다. 또한, Squaraine은 감광제의 모든 유리한 특성을 갖는 염료 계열이며 차세대 PDT의 유력한 후보로 여겨져 왔습니다. 이 연구에서 종양 특이성에 대해서는 보고되었지만, 세포 및 분자 기능에 관해 가장 연구가 적은 Squaraine N-치환된 비대칭 유도체를 선택하였습니다. 연구에서 Squaraine N-치환된 asymmetric 유도체가 인간 대장암 세포 HCT116에서 최대 광역학적 활성을 가지며 정상적인 대장 세포인 Ccd-18co에서는 세포 독성이 거의 없다는 것을 알 수 있었습니다. N-alkylated asymmetric Squaraine은 주로 mitochondria에 축적되고 mitochondria의 사멸을 유도하는 것을 알 수 있습니다.

1. Introduction

1.1. Therapy: Photodynamic Therapy (PDT)

In clinical practice, photodynamic therapy (PDT) is an innovative therapy approved for use in certain neoplastic and non-neoplastic diseases. In the case of cancer, this technique has generated great interest in the scientific community because it offers some advantages relatively to conventional treatments, namely, chemotherapy and radiotherapy.[1]

1.2. PDT: Historical Facts

PDT origin dates to ancient Egypt, Greece and India, being that these people used sunlight in combination with a photosensitizing plant to treat various skin diseases, including vitiligo and psoriasis.[2] However, it was only in the beginning of the 20th century, that PDT, as a therapeutic modality, began to develop. This is largely due to the work done by German medical student Oscar Raab, which working with Professor Herman von Tappeiner in Munich, discovered the photodynamic effect of acridine orange on protozoa and parasites in the presence of sunlight.[3] Three years later, the same group published the first treatment in patients.[4]

In the following years, the phototoxicity and fluorescence of hematoporphyrin was investigated.[5] In the 1960s, Lipson and Buckets synthesized a hematoporphyrin derivative (HpD) compound to increase tumour accumulation of the dye, and subsequently this compound was used as a fluorescent marker for diagnosis of cancer. But in 1972, Diamond *et al*. showed that HpD, besides being a diagnostic tool, could also have therapeutic applications, evidencing its efficacy in rat gliomas.[6] Subsequently, in 1975, Dougherty *et al.* demonstrated complete eradication of breast tumours in animal models after treatment with HpD.[7] In 1976, Kelly and Snell conducted the first clinical study of HpD in bladder cancer treatment. Even in this same decade, in 1978, Dougherty *et al*. have shown several successful case results obtained in patients undergoing PDT.

After these outcomes, PDT studies were intensified, and several clinical cases were published, showing PDT potentialities in the treatment of various kinds of tumours, such as bladder, brain, intraocular, pancreatic, and liver, among others.[8] Despite the promising

results of PDT in cancer treatment, it was only in 1993 that the first photosensitizer was approved in Canada, an HpD designated Photofrin®, for the treatment of bladder cancer.[9] This was, in 1995, approved by the FDA for the treatment of oesophageal cancer, and later in several countries in Europe.

1.3. PDT: Fundamentals

Photodynamic therapy consists of a therapeutic approach that requires the combination of three factors: a light source with adequate wavelength, the presence of molecular oxygen and an intermediary agent, called photosensitizer (PS), capable of absorbing and transferring energy from the light source to the oxygen, leading to the formation of reactive oxygen species (ROS), which are cytotoxic, causing damage and, consequently, cell death.[10]

In the clinical practice, the procedure consists in the administration of the photosensitizer, which should be preferentially accumulated in the tumour cells, later the excitation and activation of the photosensitizer is carried out, at the wavelength corresponding to an absorption band of PS, leading to the generation of cytotoxic species and tumour destruction.[11]

1.4. PDT: Advantages and Disadvantages

PDT has a local action, which at the same time may have advantages and disadvantages. The high selectivity of this therapy is due to the ability of many PS to accumulate preferentially in tumour cells, and because the cytotoxic action occurs only in the time interval and in the place where light interacts with the PS. Selective PS accumulation in the tumour is facilitated if the application is topical, since the PS is applied locally only on the lesion to be treated. In cases where administration is intravenous, it is necessary that the PS be kept in circulation for long enough to reach and accumulate in the tumour, taking advantage of the specific microenvironment of most solid tumours. These have fenestrated blood capillaries, reduced lymphatic drainage and low pH, which favours the passage and accumulation of the PS into the desired site.[12]

Despite the reduced systemic effects, temporary cutaneous photosensitivity reactions have been identified as the most significant adverse effect of this therapy. This is a problem that occurs due to accumulation of PS in the skin of patients. PS molecules accumulated in the skin can initiate the photodynamic reaction, by the action of sunlight or

strong artificial light, causing skin lesions or photosensitivity. The same can occur at the ocular level. To avoid this problem, patients should stay at home a few weeks after treatment, until PS levels in the skin decrease to safe values. As such, it is essential that PS have fast kinetics of elimination of the organism.[13]

The main disadvantage of the localized character of PDT is that it does not allow the treatment of metastatic tumours.[14] As such, many research groups have attempted to understand and modulate the response of the immune system, favouring a specific antitumor immune response.[15]

1.5. PDT: Light – Matter Interaction

As result of the interaction of light with matter, light energy can be transformed into other forms of energy (absorption, light emission, heat release and photochemical reactions). The search for an understanding of this interaction led to a series of studies in different areas of knowledge.

Photophysics and photochemistry are respectively concerned with describing the physical and chemical processes induced by the absorption of light, involving energetic, structural and dynamic studies. A molecule by absorbing light and being excited can lose its energy through physical processes or participate in chemical reactions. To quantify each of these processes, quantum yield (Φ) measurements are used, where Φ is the ratio of the number of photons involved in a specific process by the number of photons absorbed or number of molecules of product formed per unit of time.

1.6. PDT: Photochemistry and Photophysics

The incidence of light on a photosensitive compound can provide sufficient energy to trigger photochemical processes. When a PS, in the ground state (S_0), absorbs light, one electron is excited to a higher orbital level. This electron maintains its spin according to the spin selection rule. The excitation to a higher singlet state can be from highest occupied molecular orbital (HOMO) to lowest unoccupied molecular orbital (LUMO) or to a higher orbital, being that singlet excitation states (S_n) can have different energies (**Figure 1**). S_n>S_1 have a short lifetime (nanoseconds), so the photosensitizer rapidly loses energy to the first singlet excited state (S_1) by internal conversion (IC). From this state, the photosensitizer can experience two types of processes, one radiative and one non-radiative.[16]

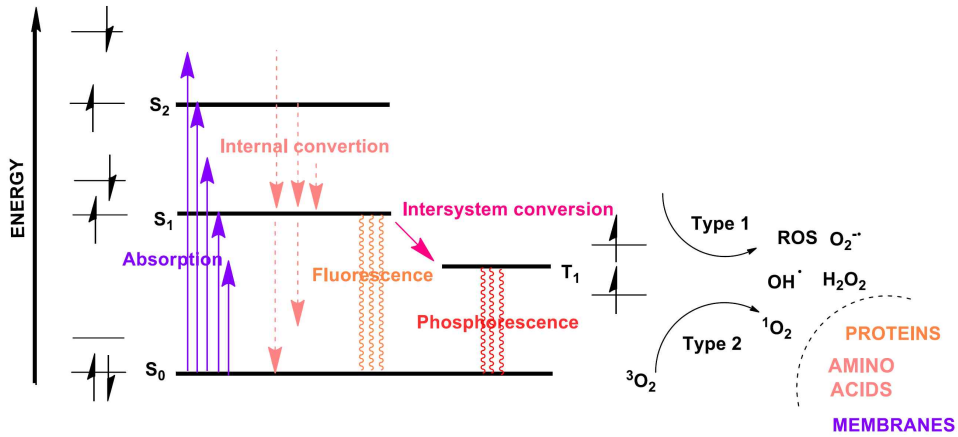

Figure 1. Perrin-Jablonski energy diagram for a photosensitizer.

In the radiative process, the photosensitizer returns to the S_0, by emission of fluorescence (**Figure 1**). Fluorescence emission is only possible in the transition from the S_1 state to the S_0 state, whereby, normally, the fluorescence wavelength is less than the excitation wavelength. The difference between the maximum excitation wavelength and the maximum emission wavelength is referred as the Stokes shift.[17] In this case the photodynamic reaction doesn't occur with therapeutic effect, however this property can potentially be used for diagnosis by obtaining fluorescence images.[18]

In the non-radiative process, the electrons undergo a spin inversion, called intersystem crossing (ISC), passing to a triplet excited state (T_1), **Figure 1**. The production of this state by the photosensitizer determines its phototherapeutic effects and the probability of triplet state formation. A high triplet state formation is required for a high efficacy of the photosensitizer in PDT. In this state (T_1), the photosensitizer may dissipate energy and return to the S_0 through a radiative emission process, referred to as phosphorescence, **Figure 1**, or may undergo quenching (nonradiative de-excitation process). The quenching mechanisms of the triplet excited state occur according to two types of photodynamic reactions, Type I and Type II, **Figure 1**.

In the Type I reaction, the photosensitizer in the T_1 state reacts directly with the substrate(s), such as cell membranes or molecules, with the transfer of an electron or a proton between them, giving rise to an anion radical or a radical cation, respectively.[19] In the presence of oxygen, and because these free radicals are highly unstable species, most react instantly to produce the superoxide anion ($O^{2-\bullet}$). In biological systems, this radical

reacts with water to produce hydrogen peroxide (H_2O_2). Hydrogen peroxide can cross cell membranes and cause damage directly on cell compartments. At higher concentrations, the superoxide anion can form highly reactive hydroxyl radicals ($^{\bullet}OH$), which attack and oxidize biological molecules.[20]

On the other hand, in the Type II reaction, the photosensitizer in the T_1 state can transfer its energy directly to the molecular oxygen, whose ground state alone is also a triplet state, producing the excited state of oxygen, the singlet oxygen ($^1O_2$). Singlet oxygen is a highly reactive species with a very short lifetime that reacts directly with biological molecules near its site of formation. Theoretically, singlet oxygen can only interact with nearby molecules and structures within its range of action.

Reactive oxygen species (ROS) formed by the photodynamic reaction are known to trigger various reactions with biomolecules including: amino acid residues in proteins, unsaturated lipids, such as cholesterol, and bases of nucleic acids. These interactions cause damage, potential destruction of cell membranes and deactivation of enzymes, inducing cell death. The singlet oxygen is considered the main cytotoxic species formed during the photodynamic process.[21] Both reactions (Type I and II) occur simultaneously, and the ratio between them depends on the type of photosensitizer used, the substrate and oxygen concentration and the amount of available oxygen. The efficiency of the Type II reaction depends on the duration (lifetime) of the triplet state and the triplet quantum yield of the photosensitizer. Both reaction types have been implicated in the efficacy of the photosensitizer and are also involved in the distinction between the two types of photodynamic reactions (Type I and II).

1.7. PDT: Characteristics of an Ideal Photosensitizer

An ideal photosensitizer for PDT must have the following characteristics: high purity and chemical stability; easy synthesis; low dark toxicity of photosensitizer and their metabolites; strong absorption in the infrared region, of the electromagnetic spectrum (600-850 nm, the so-called "therapeutic window"); have suitable photophysical characteristics such as low quantum fluorescence yield, high quantum singlet oxygen yield and a triplet state with a high half-life, as well as a partition coefficient suitable for the intended route of administration and allowing dissolution in biocompatible formulations, if necessary.[22]

1.8. PDT: Mechanisms of Tumor Cytotoxicity

Tumour destruction may occur due to direct tumour cell death, or indirectly due to injury to the tumour vasculature or induction of inflammatory reaction with subsequent immune system activation.[23]

Several clinical studies have shown that PDT may be curative, particularly in the case of non-advanced tumours. On the other hand, it is known that it can prolong survival in the case of inoperable tumours and improve the patients' quality of life.[24]

Cytotoxic effects caused by PDT *in vivo* are multifactorial and depend on the type of tumour and its level of oxygenation, the characteristics of the photosensitizer, its concentration, location at the moment of irradiation, the time between its administration and irradiation, light sources' power and total light energy received.[25] The balance of these parameters influences the extent of the various mechanisms of tumour destruction: direct destruction of tumour cells (apoptosis, autophagy or necrosis), destruction of tumour vascularization and activation of an immune response.

1.9. Direct Cytotoxicity of PDT

The direct action of PDT on tumour cells is the most studied effect when this therapeutic strategy is applied to cancer. The three main mechanisms of cell death, necrosis, apoptosis and cell death associated with autophagy can be activated in response to ROS produced in the photodynamic reaction.

Oxidative damage irreversibly destroys biomolecules and key cellular structures leading to cell death. The mechanism of cell death may be influenced by the cellular organelles where the PS molecules were located at the time of irradiation.[26]

Typically, photosensitizers located in the mitochondria or endoplasmic reticulum induce cell death by apoptosis, whereas PS located on the plasma membrane or lysosomes may induce cell death by necrosis. There is also evidence that autophagy can be induced by PDT. Autophagy is activated in an attempt by the cell to repair and survive damage to certain key organelles. If this response fails, it is transformed into a cell death signal.[27]

The known results suggest that in more aggressive PDT protocols (high doses of PS, high light doses, or both, and short times between PS administration and irradiation) tend to cause extensive necrotic cell death, unlike less intense protocols, which seem to favour cell death by apoptosis.[28]

1.10. Effect of PDT in Blood Vessels

PDT may not only have tumour cells as the targets of action. Since the early 1980s, an additional indirect mechanism coexists with the cytotoxic effect of PDT, which is the effect of vascular obstruction, which causes death by induction of ischaemia and therefore provides another pathway for the treatment of solid cancers. As such, there has been a great deal of research into the development of photosensitizing molecules both with high selectivity for tumour cells and for tumour vasculature itself.[29]

The vascular damage of PDT is because the photosensitizers are irradiated, confined in the bloodstream or accumulated in the endothelial cells or still attached to vessel walls, inducing loss of the tight junctions in the endothelial cells. These primary damages within the vessel lumen lead to thrombus formation and induce a cascade of reactions, namely, platelet aggregation, release of vasoconstricting molecules, lymphocyte adhesion, and increased vascular permeabilization. This collapse of the microvasculature associated with microhaemorrhage can cause severe hypoxia and, as such, tissue death.[30]

1.11. Immunity response to PDT

Several studies suggest that PDT induces an immune response in the host, and the innate immune system can be activated as the adaptive.[31]

Direct destruction of tumour cells, vessel occlusion, and ischemia caused often result in an acute local inflammatory reaction initiated by the secretion of proinflammatory mediators (innate immunity), such as tumour necrosis factor α (TNF-α), interleukin-1 (IL-1) or interleukin-6 (IL-6), thereby activating adaptive immunity components, such as neutrophils, mast cells, macrophages and dendritic cells, which will restore homeostasis to the region affected by the treatment (local inflammation).[32]

Crosstalk between innate immunity and adaptive immunity is established through dendritic cells (DC). DCs, when activated by inflammatory mediators, pick up the tumour antigens, and go to the nearest lymph nodes. There, they expose the antigens to CD4+ T lymphocytes, making them active. In turn, these cells activate CD8+ T lymphocytes, which recognize and destroy tumour cells.[33]

As such, in response to the photodynamic action of PDT, a local inflammatory response, as well as a systemic inflammatory response, may occur in the long term, thus allowing the eradication of metastases that are far from the irradiated site. In 2015, Rocha

et al. have developed a photosensitizer that can eliminate the primary tumour, eliciting a systemic immune response capable of controlling the metastasis.[34]

However, numerous clinical studies have demonstrated that PDT can not only trigger a stimulatory response on the immune system, as well as an immunosuppressive response.[35] The precise mechanisms that lead to each of these responses are not yet fully described, however, they are known to be related to the immune system, the treated area and the type of photosensitizer.[36] Immunosuppressive effects have only been associated with local reactions in skin lesion treatments with high irradiation areas.[37]

To improve the efficacy of clinical treatment by PDT, a greater understanding of the mechanisms associated with the immune response is needed.[38]

1.12. Squaraine Dyes

Near infrared dyes absorb light in the range of 700－1500 nm.[39] Within this range lie the first and second therapeutic windows wherein scattering as well as absorption and autofluorescence from biomolecules are minimized allowing for increased penetration of NIR light for in vivo imaging and therapeutic applications. There are relatively few classes of NIR dyes that are easily synthesized or readily available, including cyanine dyes,[40] squaraine dyes,[41] phthalocyanines,[42] porphyrins,[43] and BODIPY (borondipyrromethane)[44] analogues.

Since cyanine dyes were first discovered by C. H. Greville Williams in 1856,[45] the cyanine class has been broadly studied for various applications, such as in vivo imaging, ex vivo imaging (pH sensing and DNA stains), blood spatter analysis, and solar energy conversion.[46] Cyanine dyes consist of two heteroaromic nuclei connected by an odd-numbered chain that allows for a push/pull system between the two heterocycles. The delocalization of electrons across this bridge causes them to exhibit long wavelength absorptions.[47] Monomethine and trimethine cyanine dyes absorb in the visible range, pentamethine cyanines absorb in the near-infrared region (>700 nm), and heptamethine cyanines absorb beyond 1000 nm.[48] These dyes are widely used in semiconducting materials, laser materials, optical recording media, paints, and biological imaging applications.

Phthalocyanines are two-dimensional tetrapyrrolic macroheterocycles that contain 18 delocalized π-electrons, which are responsible for their intense absorption in the NIR region.[49]

Phthalocyanine dyes are thermally and chemically stable and highly conjugated aromatic macrocycles that have attracted interest not only for the preparation of dyes and pigments butalso as building blocks for the construction of new molecular materials for electronics and optoelectronics. In the last few years, phthalocyanines have been intensively studied as targets for optical switching and limiting devices, organic field effect transistors, sensors, light-emitting devices, low band gap molecular solar cells, optical information recording media, and photosensitizers for photodynamic therapy.[50]

The first member of the BODIPY dyes (the difluoroboraindacene family) was discovered by Treibs and Kreuzer in 1968.[51] This versatile class of dyes tend to be strongly UV absorbing small molecules that emit relatively sharp fluorescence peaks with high quantum yields.[52] They have increased in popularity over the last decades thanks to their excellent thermal and photochemical stability, high fluorescence quantum yield, negligible triplet-state formation, intense absorption profile, good solubility, and chemical robustness.[53] These attractive properties make them desirable for applications as laser dyes, molecular photonic wires, chemosensors, fluorescent switches, electron transfer reagents, and bioprobes.[54]

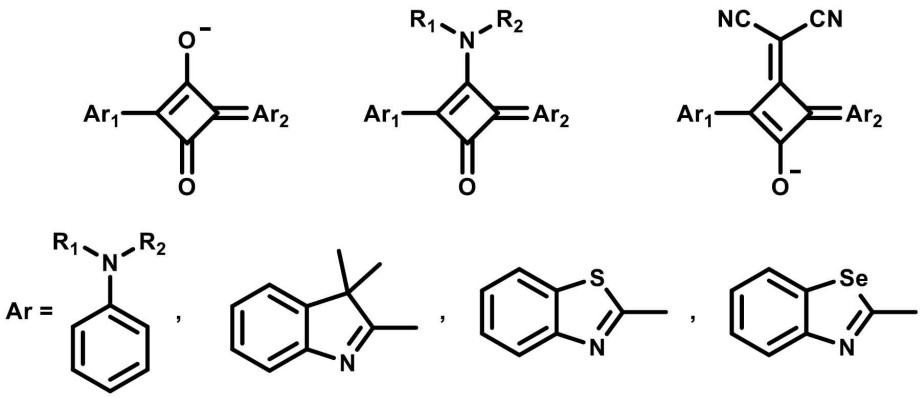

Figure 2. Common structure of Squaraine dyes.

Squaraine dyes are a class of organic dyes with an electron deficient central four-membered ring that have a resonance stabilized zwitterionic structure and were discovered by Treibs and Jacob in 1965.[55] Squaraines are derived from the highly electron deficient aromatic squaric acid core and feature electron-donating aromatic rings at diametrically opposite sides of the four-member ring. Due to their planar structures and zwitterionic properties, squaraine dyes exhibit strong absorption and emission in the NIR

region. A general structure of the squaraine chromophore is shown in **Figure 2** with Ar_1 and Ar_2 generally being electron-rich anilines or heterocycles such as trimethylindolenine, benzothiazoles, and benzoselenazoles. Additionally, the squaric core can be modified by nucleophilic substitution leading to the formation of aminosquaraine and dicyanomethylene squaraine dyes.[56]

Squaraines have extremely intense absorption bands, high molar absorption coefficient, and good photoconductivity.[57] Squaraine dyes also tend to demonstrate a narrow absorption in the NIR range, excellent photostability,[58] and high quantum yield.[59] Additionally, they are prepared through a straightforward synthetic procedure.[60] Squaraine dyes can be synthesized with functional groups providing potential sites for conjugation to enhance targeting specificity without sacrificing photophysical properties.[61] Cytotoxicity studies using various squaraines[62] and squaraine rotaxanes[63] have shown that these compounds are nontoxic even at concentrations far above the therapeutic/imaging dosages, although with significant changes to the molecular structure this may change. Therefore, squaraine dyes inherently benefit from excellent photophysical and chemical properties and are adaptable to functional groups.

1.13. Synthesis of Squaraine Dyes

1.13.1. Symmetrical Squaraine Dyes

Symmetrical squaraine dyes consist of two of the same electron-donating groups on both sides of the oxocyclobutenolate core. The starting material for the majority of squaraine dyes syntheses is squaric acid, a colorless solid. The synthesis of symmetrical squaraines is simply the condensation of two equivalents of the aryl donor groups with a single equivalent of a squaric acid acceptor. The aryl donor groups can be pyrroles, phenols, N,N-dialkyl anilines, azulenes, and activated methylene heterocycles like Fisher bases, etc.[64] For the preparation of squaraine dyes, the choice of proper conditions strongly effects the success of the reaction. Initially, Treibs and Jacob used acetic anhydride in the preparation of squaraine dyes.[65] This method was later improved by Sprenger and Ziegenbein by using a one to one mixture of butanol and benzene which allowed azeotropic removal of the byproduct water and greatly improved yields.[66] This is still the preferred method of preparing squaraines although benzene has been replaced with the less toxic toluene.[67] As illustrated in Scheme 1, the synthesis of squaraine dyes begins when

squaric acid is activated by alcohol and forms a “half ester” squarate, followed by active attack of a nucleophilic compound (Nu-H) and the subsequent loss of alcohol or acetic acid molecule. This leads to the formation of an intermediate semisquaraine. The next attack of nucleophile with the subsequent elimination of another alcohol or acetic acid molecule occurs at the 3-position and generating the symmetrical squaraine dye.

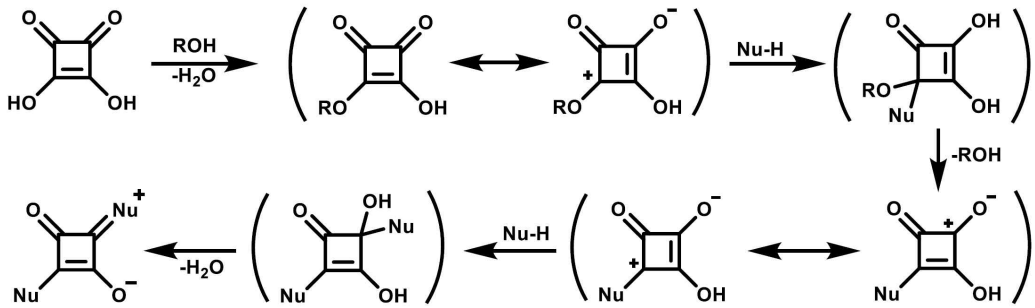

Scheme 1. Suggested Mechanism for Symmetrical Squaraine Dye Formation

1.13.2. Unsymmetrical Squaraine Dyes

Unsymmetrical squaraines contain two different substituents on the first and third carbons of the squaric acid moiety. There are two general synthetic routes to obtain unsymmetrical squaraine dyes, both starting from derivatives of squaric acid. The first strategy is using thionyl chloride or oxalyl chloride to prepare 3,4-dichlorocyclobut-3-ene-1,2-dione,[68] with the subsequent addition of one equivalent of an activated aromatic compound, followed by immediate hydrolysis to obtain the intermediate semisquaraine, as shown in Scheme 2. Then the semisquaraine is then allowed to react with a different aromatic compound to afford the final unsymmetrical structure.

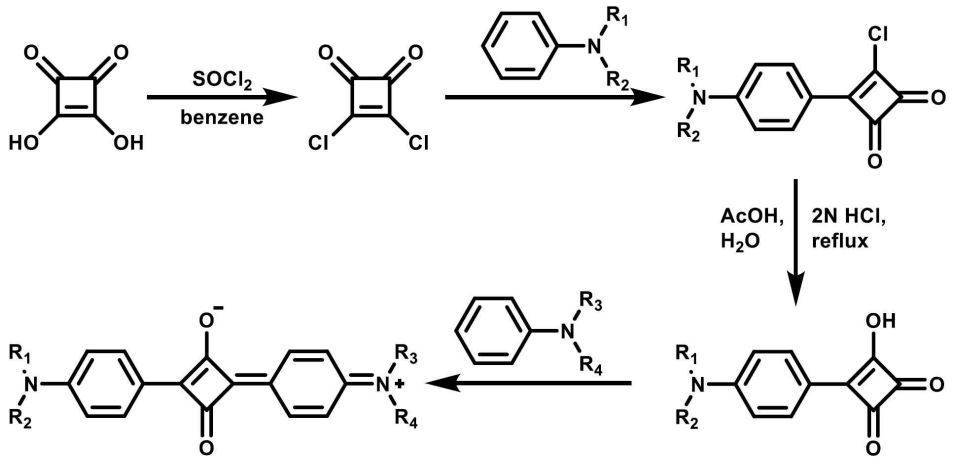

Scheme 2. Synthesis of Unsymmetrical Squaraine Dyes Using Thionyl Chloride

In the second strategy, unsymmetrical squaraine dyes containing more reactive N-alkylated heterocyclic structures such as alkyl-indolinium, alkyl-benzothiazolium, and alkylquinolinium salts can be synthesized through the use of 3,4-dialkoxy-cyclobut-3-ene-1,2-dione, as shown in Scheme 3.[69] Activated heterocyclic compounds react with 3,4-dialkoxycyclobut-3-ene-1,2-dione in a 1:1 ratio in ethanol with triethylamine (TEA), resulting in the semisquaraine intermediate. The semisquaraine is then reacted with another heterocyclic compound, generating the anticipated unsymmetrical structure. However, the regioselectivity should not be ignored during condensation of semisquaraine with the second equivalent of donor. During the reaction, the 1,2-condensation byproduct can be formed along with the desired 1,3-condensation product.[70]

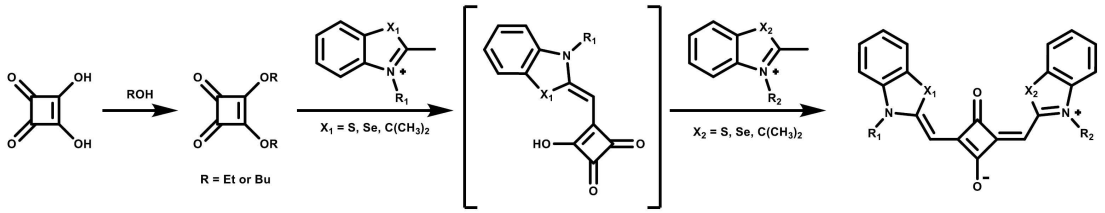

Scheme 3. Synthesis of Unsymmetrical Squaraine Dyes with N-Alkylated Heterocyclic Structures.

2. Experimental Section

2.1. General considerations

All manipulations were performed under either a dry nitrogen atmosphere using either standard Schlenk techniques. Ethanol, and acetic acid were purchased from Samchun Pure Chemical Company and used without further purification. Acetonitrile was dried over sodium/benzophenone before use. Glassware, syringes, magnetic stirring bars, and needles were dried overnight in a convection oven. 4-Bromoaniline, 3-methylbut-2-one, iodoethane, iodobutane, iodohexane, 3,4-dihydroxycyclobut-3-ene-1,2-dione, n-butanol, tin (II) chloride dihydrate, and triethylamine were purchased from Aldrich Chemicals. All compounds were synthesized by modified literature procedure.[37] IR spectra were recorded on an Agilent Cary 600 Series FT-IR spectrometer using KBr disks. The ^{1}H and ^{13}C NMR spectra were recorded on a Bruker 300 spectrometer operating at 300.1 and 75.4 MHz, respectively. All ^{1}H and ^{13}C NMR chemical shifts were measured relative to the internal residual $CHCl_3$ from the lock solvent (99.9% $CDCl_3$). Reactions were monitored by thin-layer chromatography (TLC) on aluminium plates with 0.25 mm of silica gel (TLC Silicagel 60 F254, Merck, Darmstadt, Germany), which were, whenever necessary, visualized by UV detection. Purification by column chromatography was carried out on silica gel 60 (70−230 mesh) using a mixture of ethyl acetate and petroleum ether (1:1) or CH_2Cl_2 as eluent. Elemental analyses (Carlo Erba Instruments CHNS-O EA1108 analyzer) were performed by the Ochang branch of the Korean Basic Science Institute. All melting points were uncorrected.

2.2. In Vitro Cytotoxicity Evaluation

The cytotoxicity of compounds **3a**, **3b**, **3c**, **4a**, **4b**, and **4c** to C6 glioma cell line (rat brain cancer cell) was assessed by the MTT cell viability assay. In summary, C6 glioma cells were seeded into a 96-well microplate at a density of 5×10^4cells/well in 100 μL of Ham's F-12 medium, supplemented with 10% fetal bovine serum (FBS), and allowed to adhere overnight at 37°C in 5% CO_2. The medium was then replaced with the same

volume of Ham's F-12 containing different concentrations (0−10 μM) of compounds **3a**, **3b**, **3c**, **4a**, **4b**, and **4c** and afterward, cytotoxicity was assessed in 2 h incubation at 37 °C for 4 h in the dark after addition of compounds **3a**, **3b**, **3c**, **4a**, **4b**, and **4c**. Then, the cells were washed twice with PBS, and 100 μL of MTT (5 mg/mL in PBS) was added to each well and the plates were incubated at 37 °C for 4 h in the dark. The medium was removed and 200 μL of DMSO was added to dissolve the blue formazan crystals for 20 min. The absorbance was read on an ELISA Reader at 540 nm. The relative cell viability was calculated by dividing the mean optical density value of the control group, and the average value was obtained from six parallel samples. The effect of UV irradiation was investigated after treating of C6 glioma cells with the aforementioned compounds in a range of concentrations from 0 to 10 μM for 2 h at 37 °C in 5% CO_2 and then exposing them to UV lamp (365nm) with a 10 cm distance for 3 min. Immediately after UV irradiation and illumination with greenligh (532nm) for 90 s, the cell viability was measured using the technique mentioned before. All experiments were performed in triplicate.

2.3. Synthesis

2.3.1. Synthesis of (*E*)-3-[(1-ethyl-3,3-dimethylindolin-2-ylidene)methyl]-4-butoxycyclobut-3-ene-1,2-diones (1a)

General Procedure. 2,3,3-Trimethyl-2-methyleneindoline (7.9 g, 20.0 mmol) and 1.2 equiv of 3,4-dibutoxycyclobut-3-ene-1,2-dione (5.4 g, 22.0 mmol) with 22.0 mmol of NEt_3 dissolved in anhydrous ethanol (50 mL) and the mixture was stirred at 25 °C for 7 h. The progress of the reaction was monitored by thin layer chromatography. After completion of the reaction, the removal of the solvent at the rotary evaporator gave a crude product, which was then extract with Et_2O at 3 times. The combined organic layer concentrated by rotary evaporator then recrystallized in EtOH to yield **1a**. Yield: 19%, (0.13 g, 0.38 mmol). M.P. 76 − 77 °C. Elemental Analysis : $C_{21}H_{25}NO_3$, Found : C, 74.31; H, 7.42; N, 4.13; O, 14.14. ^{1}H NMR ($CDCl_3$-*d*) δ 0.96 (t, 3H, C*H*$_3$), 1.33 (m, 2H, *C*H$_2$), 1.66 (m, 2H, *C*H$_2$), 1.49 (d, indoline *C*H$_3$), 3.10 (q, N−*C*H$_2$), 3.96 (m, O−*C*H$_2$), 5.64 (s, C−*H*), 6.35 (m, 1H, indoline C−*H*), 6.50 (m, 1H, indoline C−*H*), 6.91 (m, 1H, indoline C−*H*), 6.86 (m, indoline

C−*H*). ^{13}C NMR ($CDCl_3$-*d*) δ 13.4, 14.1, 26.8 (*C*H_3), 19.2, 32.4 (*C*H_2), 47.9 (N−*C*H_2), 51.1 (=*C*−*C*), 65.9 (O−*C*H_2), 94.9, 172.8 (*C*=*C*), 113.2, 116.9, 126.8, 127.0 140.9, 144.1 (indoline ring), 128.3, 176.2 (*C*=*C*), 187.0 (*C*=O).

1b: Yield: 15% (0.11 g, 0.4 mmol). M.P. 79 − 80 °C. Elemental Analysis : $C_{23}H_{29}NO_3$, Found : C, 75.17; H, 7.95; N, 3.81; O, 13.06. ^{1}H NMR ($CDCl_3$-*d*) δ 0.96 (t, 3H, C*H*$_3$), 1.33 (m, 2H, *C*H_2), 1.52 (m, 2H, *C*H_2), 1.66 (m, 2H, *C*H_2), 1.47 (d, indoline *C*H_3), 3.06 (q, N−*C*H_2), 3.96 (m, O−*C*H_2), 5.62 (s, C−*H*), 6.33 (m, 1H, indoline C−*H*), 6.48 (m, 1H, indoline C−*H*), 6.79 (m, 1H, indoline C−*H*), 6.84 (m, indoline C−*H*). ^{13}C NMR ($CDCl_3$-*d*) δ 13.8, 14.1, 27.0 (*C*H_3), 19.2, 32.4, 30.6, 44.9 (*C*H_2), 44.8 (N−*C*H_2), 51.2 (=*C*−*C*), 65.9 (O−*C*H_2), 95.0, 172.9 (*C*=*C*), 113.3, 117.0, 126.7, 127.1 141.0, 144.2 (indoline ring), 128.3, 176.2 (*C*=*C*), 187.0, (*C*=O).

1c: Yield: 17% (0.13 g, 0.34 mmol). M.P. 78 − 79 °C. Elemental Analysis : $C_{25}H_{33}NO_3$, Found : C, 75.91; H, 8.41; N, 3.54; O, 12.14. ^{1}H NMR ($CDCl_3$-*d*) δ 0.96 (t, 3H, C*H*$_3$), 1.29 (m, 2H, *C*H_2), 1.33 (m, 2H, *C*H_2), 1.52 (m, 2H, *C*H_2), 1.65 (m, 2H, *C*H_2), 1.46 (d, indoline *C*H_3), 3.06 (q, N−*C*H_2), 3.95 (m, O−*C*H_2), 5.61 (s, C−*H*), 6.32 (m, 1H, indoline C−*H*), 6.47 (m, 1H, indoline C−*H*), 6.88 (m, 1H, indoline C−*H*), 6.83 (m, indoline C−*H*). ^{13}C NMR ($CDCl_3$-*d*) δ 45.1 (N−*C*H_2), 14.1, 14.3 (*C*H_3), 19.4, 22.8, 26.9, 27.2, 28.4, 31.6, 32.6 66.1 (*C*H_2), 66.3 (O−*C*H_2), 51.3 (=*C*−*C*), 95.1, 173.0 113.1, 116.8, 126.7, 126.1 140.8, 144.0 (indoline ring), (*C*=*C*), 128.5, 176.4 (*C*=*C*), 187.1 (*C*=O).

2a: Yield: 15% (0.12 g, 0.3 mmol). M.P. 75 − 76 °C. Elemental Analysis : $C_{21}H_{24}BrNO_3$, Found: C, 60.29; H, 5.78; Br, 19.10; N, 3.35; O, 11.47. ^{1}H NMR ($CDCl_3$-*d*) δ ^{1}H NMR ($CDCl_3$-*d*) δ 0.96 (t, 3H, C*H*$_3$), 1.34 (m, 2H, *C*H_2), 1.68 (m, 2H, *C*H_2), 1.50 (d, indoline *C*H_3), 3.11 (q, N−*C*H_2), 3.97 (m, O−*C*H_2), 5.65 (s, C−*H*), 7.08 (m, 1H, indoline C−*H*), 7.03 (m, indoline C−*H*), 6.24 (m, 1H, indoline C−*H*). ^{13}C NMR ($CDCl_3$-*d*) δ 13.6, 14.1, 26.9, 26.9 (CH_3), 19.5, 32.7 (*C*H_2), 48.1 (N−*C*H_2), 51.2 (=*C*−*C*), 66.1 (O−*C*H_2), 95.1, 173.0 (*C*=*C*), 111.2, 115.4, 129.7, 131.7, 143.1 (indoline ring), 128.5, 176.4 (*C*=*C*), 187.0 (*C*=O).

2b: Yield: 17% (0.15 g, 0.34 mmol). M.P. 77 − 78 °C. Elemental Analysis :$C_{23}H_{28}BrNO_3$, Found: C, 61.89; H, 6.32; Br, 17.90; N, 3.14; O, 10.95. ^{1}H NMR ($CDCl_3$-*d*) δ ^{1}H NMR ($CDCl_3$-*d*) δ 0.96 (t, 3H, C*H*$_3$), 1.33 (m, 2H, *C*H$_2$), 1.52 (m, 2H, *C*H$_2$), 1.67 (m, 2H, *C*H$_2$), 1.51 (d, indoline *C*H$_3$), 3.06 (q, N−*C*H$_2$), 3.98 (m, O−*C*H$_2$), 5.66 (s, C−*H*), 6.26, 7.10 (m, 1H, indoline C−*H*), 7.05 (m, indoline C−*H*). ^{13}C NMR ($CDCl_3$-*d*) δ 13.8, 14.1, 27.3 (*C*H$_3$), 19.7, 20.6, 31.0, 32.9 (*C*H$_2$), 44.8 (N−*C*H$_2$), 51.6 (=*C*−*C*), 66.3 (O−*C*H$_2$), 95.5, 173.4 (*C*=*C*), 111.6, 115.8, 130.1, 132.1, 143.4, 143.5 (indoline ring), 128.7, 176.6 (*C*=*C*), 187.0 (*C*=O).

2c: Yield: 18% (0.18 g, 0.38 mmol). M.P. 80 − 81 °C. Elemental Analysis : $C_{25}H_{32}BrNO_3$, Found: C, 63.29; H, 6.80; Br, 16.84; N, 2.95; O, 10.12. ^{1}H NMR ($CDCl_3$-*d*) δ ^{1}H NMR ($CDCl_3$-*d*) δ 0.97 (t, 3H, C*H*$_3$). 1.29 (m, 2H, *C*H$_2$), 1.33 (m, 2H, *C*H$_2$), 1.36 (m, 2H, *C*H$_2$), 1.52 (m, 2H, *C*H$_2$), 1.68 (m, 2H, *C*H$_2$), 1.53 (d, indoline *C*H$_3$), 3.07 (q, N−*C*H$_2$), 3.99 (m, O−*C*H$_2$), 5.67 (s, C−*H*), 6.27 (m, indoline C−*H*), 7.06 (m, indoline C−*H*), 7.11 (m, 1H, indoline C−*H*). ^{13}C NMR ($CDCl_3$-*d*) δ 14.2, 27.4 (*C*H$_3$), 19.8, 22.8, 2.72, 28.4, 31.6, 33.0 (*C*H$_2$), 51.7 (=*C*−*C*), 45.1 (N−*C*H$_2$), 66.4 (O−*C*H$_2$), 95.6, 173.5 (*C*=*C*), 111.7, 115.9, 130.2, 132.2, 143.6, 143.5 (indoline ring), 128.8, 176.7 (*C*=*C*), 187.1, 187.1 (*C*=O).

2.3.2. Synthesis of 4-[(*E*)-(1-ethyl-3,3-dimethylindolin-2-ylidene)methyl]-2-[(*E*)-(1-butyl-3,3-dimethylinolin-2-ylidene)methyl]-3-oxocyclobut-1-enone (3a)

General Procedure. **1a** (2.82 g, 10.0 mmol) and 1.2 equiv of 1-butyl-2,3,3-trimethyl-3*H*-inolium iodide (4.11 g, 12.0 mmol) with 12.0 mmol of n-butanol dissolved in anhydrous toulene (50 mL) and the mixture was stirred at 120 °C for 12 h. The progress of the reaction was monitored by thin layer chromatography. After completion of the reaction, the removal of the solvent at the rotary evaporator gave a crude product, which was then column chromatographed (SiO2, EA:Hx 2:1) to yield **3a**. Yield: 13%, (0.12 g, 0.26 mmol). M.P. 78 − 79 °C. Elemental Analysis : $C_{32}H_{37}N_2O_2$, Found : C, 79.80; H, 7.74; N, 5.82; O, 6.64. ^{1}H NMR ($CDCl_3$-*d*) δ 0.96 (t, 3H, C*H*$_3$), 1.33 (m, 2H, *C*H$_2$), 1.52 (m, 2H, *C*H$_2$), 1.49 (d, indoline *C*H$_3$), 3.06 (q, N−*C*H$_2$), 3.10 (q, N−*C*H$_2$), 3.72 (m, C−*H*), 5.09 (s, C−*H*), 5.64 (s, C−*H*), 6.35 (m, 1H, indoline C−*H*), 6.50 (m, 1H, indoline C−*H*),

6.91 (m, 1H, indoline C−*H*), 6.86 (m, indoline C−*H*). ^{13}C NMR ($CDCl_3$-*d*) δ 13.4, 13.8, 20.6, 26.7, 26.8, 30.6 (*C*H_3), 44.8, 47.8 (N−*C*H_2), 47 (=*C*−*C*, squaraine), 51.1 (=*C*−*C*), 90.7, 94.9, 151.0, 172.8 (*C*=*C*), 113.2, 116.9, 126.8, 127.0 140.9, 144.1 (indoline ring), 130 (=*C*−O, squaraine), 144 (*C*=*C*, squaraine), 196.5 (−*C*=O, squaraine).

3b: Yield: 10% (0.1 g, 0.2 mmol). M.P. 80 − 81 °C. Elemental Analysis : $C_{34}H_{41}N_2O_2$, Found: C, 80.12; H, 8.11; N, 5.50; O, 6.28. ^{1}H NMR ($CDCl_3$-*d*) δ 0.96 (t, 3H, C*H*$_3$), 1.31 (m, 2H, *C*H_2), 1.35 (m, 2H, *C*H_2), 1.54 (m, 2H, *C*H_2), 1.53 (d, indoline *C*H_3), 3.08 (q, N−*C*H_2), 3.12 (q, N−*C*H_2), 3.70 (m, C−*H*), 5.11 (s, C−*H*), 5.66 (s, C−*H*), 6.37 (m, 1H, indoline C−*H*), 6.52 (m, 1H, indoline C−*H*), 6.93 (m, 1H, indoline C−*H*), 6.88 (m, indoline C−*H*). ^{13}C NMR ($CDCl_3$-*d*) δ 13.4, 14.1, 26.7, 26.8 (*C*H_3), 22.8, 27.2, 28.4, 31.6 (*C*H_2), 45.1, 47.8 (N−*C*H_2), 47.2 (=*C*−*C*, squaraine) 51.1 (=*C*−*C*), 90.7, 94.9, 151.0, 172.8 (*C*=*C*), 113.5, 117.2, 127.1, 127.3 141.2, 144.4 (indoline ring), 131 (=*C*−O, squaraine), 145 (*C*=*C*, squaraine), 196.8 (−*C*=O, squaraine).

3c: Yield: 11% (0.12 g, 0.22 mmol). M.P. 79 − 80 °C. Elemental Analysis : $C_{32}H_{37}N_2O_2$, Found : C, 80.41; H, 8.43; N, 5.21; O, 5.95. ^{1}H NMR ($CDCl_3$-*d*) δ 0.96 (t, 3H, C*H*$_3$), 1.30 (m, 2H, *C*H_2), 1.35 (m, 2H, *C*H_2), 1.53 (m, 2H, *C*H_2), 1.50 (d, indoline *C*H_3), 3.07 (q, N−*C*H_2), 3.75 (m, C−*H*), 5.08 (s, C−*H*), 5.66 (s, C−*H*), 6.36 (m, 1H, indoline C−*H*), 6.51 (m, 1H, indoline C−*H*), 6.92 (m, 1H, indoline C−*H*), 6.87 (m, indoline C−*H*). ^{13}C NMR ($CDCl_3$-*d*) δ 14.2, 14.3, 26.8, (*C*H_3), 20.9, 23.2, 27.5, 28.7, 30.9, 31.9 (*C*H_2), 44.7, 45.3 (N−*C*H_2), 47.5 (=*C*−*C*, squaraine), 51.1, 51.3 (=*C*−*C*), 94.9, 90.9, 151.2, 172.8 (*C*=*C*), 113.4, 117.1, 126.9, 127.1 141.9, 144.0 (indoline ring), 130.5 (=*C*−O, squaraine), 144.4 (*C*=*C*, squaraine), 196.6 (−*C*=O, squaraine).

4a: Yield: 16% (0.2 g, 0.32 mmol). M.P. 80 − 81 °C. Elemental Analysis : $C_{32}H_{35}Br_2N_2O_2$, Found: C, 60.11; H, 5.52; Br, 24.99; N, 4.38; O, 5.00. ^{1}H NMR ($CDCl_3$-*d*) δ 0.96 (t, 3H, C*H*$_3$), 1.33 (m, 2H, *C*H_2), 1.52 (m, 2H, *C*H_2), 1.49 (d, indoline *C*H_3), 3.06(q, N−*C*H_2), 3.10 (q, N−*C*H_2), 3.72 (m, C−*H*), 5.09 (s, C−*H*), 5.64 (s, C−*H*), 6.24 (m, 1H, indoline C−*H*), 6.35 (m, 1H, indoline C−*H*), 7.08 (m, 1H, indoline C−*H*), 7.03 (m, indoline C−*H*). ^{13}C NMR ($CDCl_3$-*d*) δ 13.4, 13.8, 26.7, 26.8 (*C*H_3), 20.6, 30.6 (*C*H_2), 47 (=*C*−*C*,

squaraine), 44.8, 47.8 (N−CH_2), 50.4, 51.1 (=*C*−*C*), 90.7, 94.9, 151.0, 172.8 (*C*=*C*), 111.4, 115.5, 129.9, 131.8 143.2, 143.2 (indoline ring), 130 (=*C*−O, squaraine), 144 (*C*=*C*, squaraine), 196.5 (−*C*=O, squaraine).

4b: Yield: 12% (0.16 g, 0.24 mmol). M.P. 79 − 80 °C. Elemental Analysis : $C_{34}H_{39}Br_2N_2O_2$, Found: C, 61.18; H, 5.89; Br, 23.94; N, 4.20; O, 4.79. ^{1}H NMR ($CDCl_3$-*d*) δ 0.98 (t, 3H, CH_3), 12.9 (m, 2H, *C*H_2), 1.36 (m, 2H, *C*H_2), 1.55 (m, 2H, *C*H_2), 1.51 (d, indoline *C*H_3), 3.08 (q, N−*C*H_2), 3.13 (q, N−*C*H_2), 3.73 (m, C−*H*), 5.09 (s, C−*H*), 5.68 (s, C−*H*), 6.35 (m, 1H, indoline C−*H*), 7.11 (m, 1H, indoline C−*H*), 7.06 (m, indoline C−*H*). ^{13}C NMR ($CDCl_3$-*d*) δ 12.4, 14.1, 22.4, 25.7 (*C*H_3), 22.8, 27.2, 28.4, 31.6 (*C*H_2), 45.8, 46.8 (N−*C*H_2), 47.2 (=*C*−*C*, squaraine), 50.1, 50.9 (=*C*−*C*), 90.2, 93.9, 150.5, 171.8 (*C*=*C*), 110.2, 114.4, 128.7, 130.7 142.1, 142.1 (indoline ring), 130.2 (=*C*−O, squaraine), 144.5 (*C*=*C*, squaraine), 196.8 (−*C*=O, squaraine).

4c: Yield: 19% (0.26 g, 0.38 mmol). M.P. 80 − 81 °C. Elemental Analysis : $C_{36}H_{43}Br_2N_2O_2$, Found : C, 62.16; H, 6.23; Br, 22.98; N, 4.03; O, 4.60. ^{1}H NMR ($CDCl_3$-*d*) δ 0.92 (t, 3H, CH_3), 1.24 (m, 2H, *C*H_2), 1.36 (m, 2H, *C*H_2), 1.37 (m, 2H, *C*H_2), 1.55 (m, 2H, *C*H_2), 1.56 (m, 2H, *C*H_2), 1.51 (d, indoline *C*H_3), 3.08 (q, N−*C*H_2), 3.76 (m, C−*H*), 5.02 (s, C−*H*), 5.68 (s, C−*H*), 6.38, 7.09 (m, 1H, indoline C−*H*), 7.06 (m, indoline C−*H*). ^{13}C NMR ($CDCl_3$-*d*) δ 14.1, 14.3, 26.8, 26.9 (*C*H_3), 20.8, 22.9, 27.5, 28.6, 30.9, 31.8 (*C*H_2), 44.9, 45.8 (N−*C*H_2), 46.6 (=*C*−*C*, squaraine), 50.8 (=*C*−*C*), 90.9, 95.9, 151.8, 173.8 (*C*=*C*), 111.6, 115.7, 123.1, 131.9 143.4, 143.4 (indoline ring), 131.2 (=*C*−O, squaraine), 145.6 (*C*=*C*, squaraine), 197.3 (−*C*=O, squaraine).

3. Results and Discussion

3.1. Synthesis of mono-indolinium substituted squaraine derivatives (1a – 2c)

The synthetic route used to prepared (*E*)-3-[(5-bromo-1-alkyl-3,3-dimethylindolin-2-ylidene)methyl]-4-butoxycyclobut-3-ene-1,2-diones is depicted in Scheme 4. The 1a – 2c are prepared in moderate yield from 1-alkyl-2,3,3-trimethyl-2-methyleneindolinium iodide salt and 1.2 equiv of 3,4-dibutoxycyclobut-3-ene-1,2-dione in anhydrous ethanol at room temperature for 7 h. The synthesis of N-alkylated indolium iodide salt has been describe previous using a somewhat more complicated method. The relatively electron withdrawing and steric effect of the iodide than bromide activated alkyl iodide to such an extent that it reacts more fast with 2,3,3-trimethylindole as starting material in the ethanol solvent to give target compound. However, as the alkyl chain in the alkyl iodide precursor increases in length, the temperature and reaction time required to complete the reaction also increases.

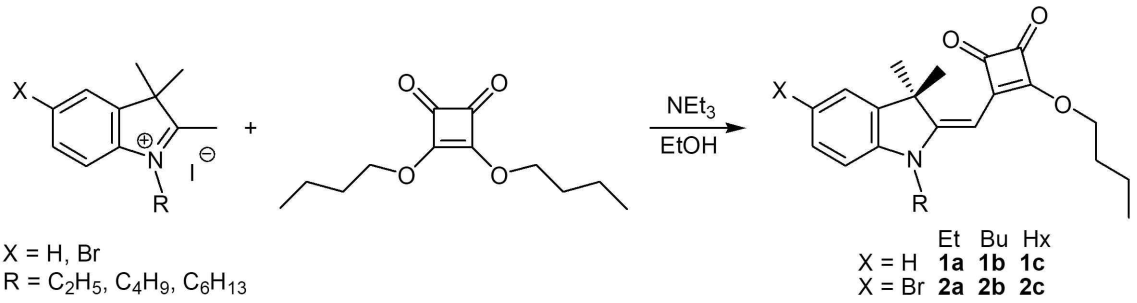

Scheme 4. Synthesis of spiropyrane derivatives **1a** – **2c**.

Reaction of 1-alkyl-2,3,3-trimethylindolin-2-ylidenium iodide salt with 1.2 equiv of 3,4-dibutoxycyclobut-3-ene-1,2-dione in ethanol with triethylamine (NEt3) affords the (*E*)-3-[(5-bromo-1-alkyl-3,3-dimethylindolin-2-ylidene)methyl]-4-butoxycyclobut-3-ene-1,2-diones in moderate yields (**1a** 19%, **1b** 15%, **1c** 17%, **2a** 15%, **2b** 17%, **2c** 18%), respectively. The disappearances of the starting materials was monitored by TLC. For mono-substituted

squaraine derivatives were diluted with Et_2O and then washed with distilled H_2O. The combined orgainc layer evaporated by rotary evaporator then purified by recrystallization in cold ethanol. They are stable in air and showed no signs of decomposition up to room temperature.

The mono-substituted squaraine derivatives were characterized using 1H, and 13C nuclear magnetic resonance (NMR) spectroscopy. The ^{1}H NMR spectra of **1a – 2c** show resonances at around δ = 1.29 – 1.68 ppm due to the methyl proton in the $-CH_3$ and $N-CH_2$ unit and at around δ = 3.00 – 3.11 ppm, 3.95 – 3.97 ($O-CH_2$). The ^{13}C NMR spectra of **1a – 2c** exhibit resonances at around δ = 14 – 27 ($-CH_3$), 44 – 45 ($N-CH_2$), 95 – 173 (*C*=*C*), 187 (*C*=O), 66 – 67 ($O-CH_2$) and 113 – 144 (indoline ring).

3.2. Synthesis of unsymmetrical di-indolium substituted squaraine derivatives (3a – 4c)

A similar protocol was applide to the preparation of unsymmetrical di-indolium substituted squaraine derivatives as shown in Scheme 5. The unsymmetrical di-indolium substituted squaraine derivatives prepared from 1a – 2c with N-alkylated 2,3,3-trimethylindole and n-butanol using an analogous method. For target compounds, 4-[(*E*)-(5-bromo-1-R_1-3,3-dimethylindolin-2-ylidene)methyl]-2-[(*E*)-(5-bromo-1-R_2-3,3-dimethylindolin-2-ylidene)methyl]-3-oxocyclobut-1-enones (**3a – 4c**) were filtered off with silica gel in order to remove the impurities formed during the carbon-carbon coupling reaction, then washed with cold ethanol. The target compounds are powder form at room temperature and were further purified by column chromatography (EA:Hx 2:1). They are stable in air and showed no signs of decomposition up to room temperature.

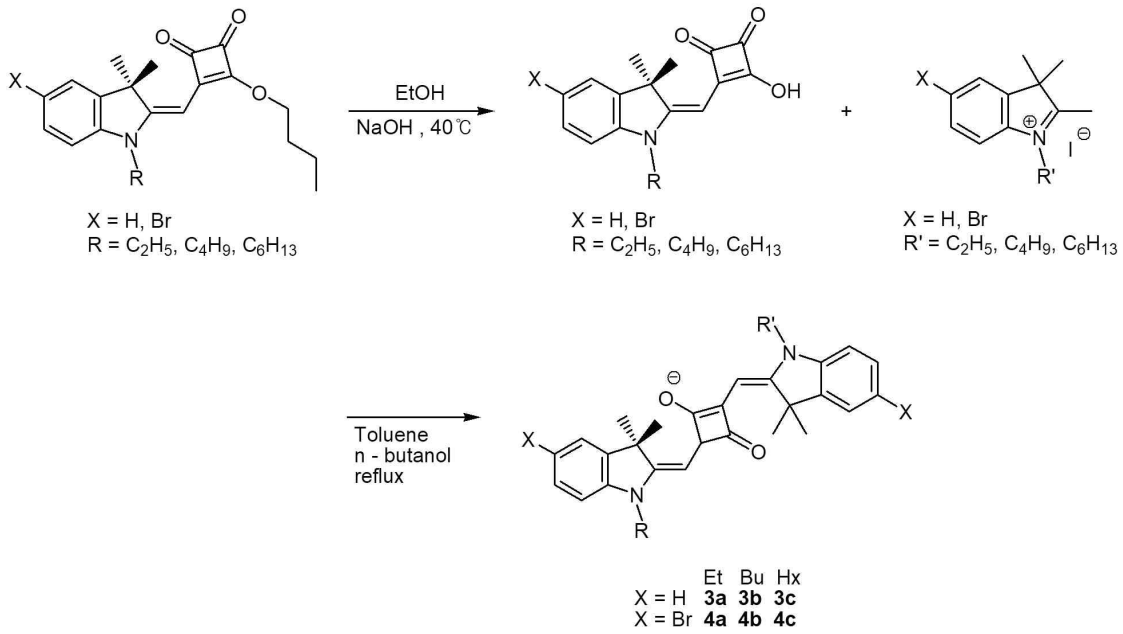

Scheme 5. Synthesis of N-alkylated spiropyran derivatives **4** − **6.**

The **3a** – **4c** were characterized using ^{1}H and ^{13}C nuclear magnetic resonance (NMR) spectroscopy. The most noteworthy feature of the ^{1}H NMR spectra of the **3a** – **4c** is the characteristic resonance for the neutral N–CH_2 and N–CH_2 cation protons. In most compounds this proton is observed at around 44 – 45 ppm, but no clear trends are present.

3.3. Biological activity of unsymmetrical squaraine derivatives

All the synthesized unsymmetrical squaraine derivatives were screened for their in vitro cytotoxicity. All tested unsymmetrical squaraine derivatives in the present study with a chain length of C_2, C_4, and C_6 at the N-position consistently show higher cytotoxicity–*i.e.* lower IC_{50} values–than the corresponding increasing carbon number. Among the ethyl-butyl substituted unsymmetrical squaraine derivatives (**3a** and **4a**) are less cytotoxicity within the tested concentration range with an IC_{50} value around 1000 μM. A relatively high

cytotoxicity was found for the butyl-hexyl substituted unsymmetrical squaraine derivatives (**3c** and **4c**) as shown in Figure 2 and 3. This suggests an intrinsic cytotoxicity effect of the well known side chain length effect of the nitrogen atom was supported by our results when looking at unsymmetrical squaraines of which all three different side chains were tested.

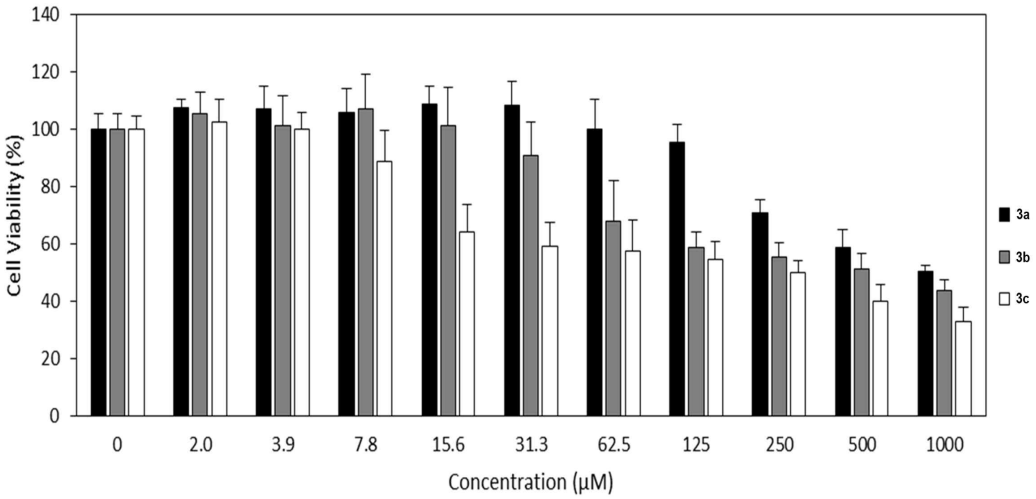

Figure 2. Cytotoxicity evaluation of **3a** – **3c** for HCT116 cancer cells.

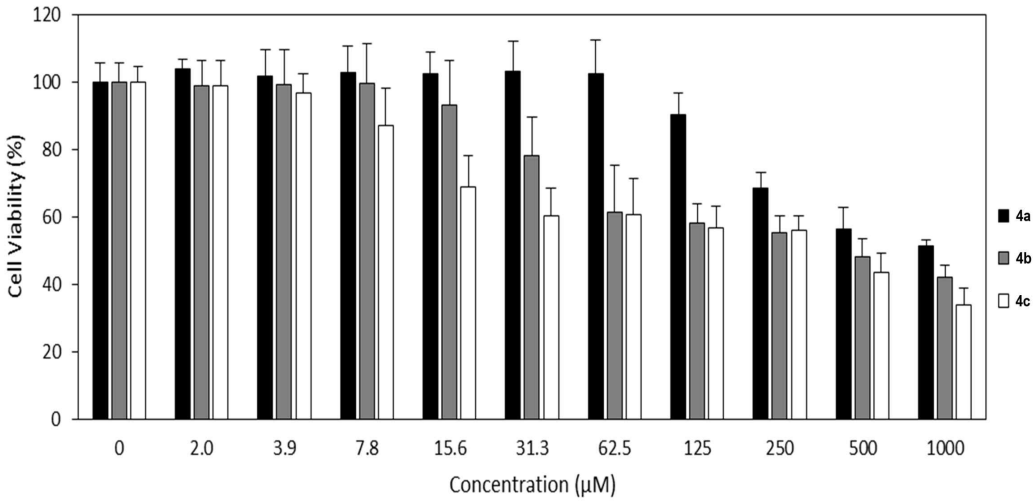

Figure 3. Cytotoxicity evaluation of **4a** – **4c** for HCT116 cancer cells.s

The cytotoxicity of the unsymmetrical squaraine derivatives are normalized with various alkyl chain lengths. The results obtained in our study are discussed along to the following

questions: (i) Can the impact of the alkyl chain be attributed to physical and/or chemical properties of the compounds and if so, which mode of action might be responsible for the observed cytotoxic effect? (ii) Can the impact of the alkyl chain lengths be explained by the intrinsic cytotoxicity of the squaraines? (iii) Is a simple model of mixture toxicity helpful in predicting the cytotoxicity of unsymmetrical squaraine derivatives that have not been investigated yet?

The presented results clearly demonstrate that anions can influence the cytotoxicity of unsymmetrical squaraine derivatives. In the following section the alkyl chain lengths exhibiting a significant effect are analyzed in detail using the various programs to elucidate physical and/or chemical properties that are responsible for the observed unsymmetrical squaraine derivatives cytotoxicity.

4. Conclusions

In summary, we have synthesized six water soluble unsymmetrical squaraine derivatives having very good extinction coefficient ranging in the order of 104 − 105 in the phototherapeutic window. Presence of *N*-alkylated dimethylindole moieties in these molecules can improve its intersystem crossing efficiency to the triplet state as refluxed from their good triplet quantum yield and a long triplet lifetime. Good triplet excited properties combined with the presence of indole groups allow to study the in vitro cytotoxic effect in live cells by MTT exclusion method.

In general, the model-based prospective estimation of the cytotoxicity combined with experimentally derived cytotoxicity data for anions and cations complemented by consideration of structure-property relationships opens up the opportunity to overcome the above mentioned dilemma of an unmanageable pool of possible ionic liquids.

In this iterative approach chemists creativity is guided by the structural properties of cation and anion species, which leads to a reduced number of task specific and intrinsically safer ionic liquids. Through such a process more sustainable ionic liquids can be realized.

5. References

1. Bonnett, R. (2000A) Chemical Aspects of Photodynamic Therapy. Gordon and Breach Science Publishers, Amsterdam.

2. Bonnet, R. (1995) Photosensitizers of the porphyrin and phthalocyanine series for photodynamic therapy. Chem. Soc. Rev. 24, 19–33.

3. Kubler, A. C. (2005) Photodynamic therapy. Med. Laser Appl. 20, 37–45.

4. Robertson, C. A., D. H. Evans and H. Abrahamse (2009) Photodynamic therapy (PDT): A short review on cellular mechanisms and cancer research applications for PDT. J. Photochem. Photobiol., B 96, 1–8.

5. Redmond, R. W. and I. E. Kochevar (2006) Spatially resolved cellular responses to singlet oxygen. Photochem. Photobiol. 82, 1178–1186.

6. Ogilby, P. R. (2010) Singlet oxygen: There is indeed something new under the sun. Chem. Soc. Rev. 39, 3181–3209.

7. Sanabria, L. M., M. E. Rodrıguez, I. S. Cogno, N. B. R. Vittar, M. F. Pansa, M. J. Lamberti and V. A. Rivarola (2013) Direct and indirect photodynamic therapy effects on the cellular and molecular components of the tumor microenvironment. Biochim. Biophys. Acta 1835, 36–45.

8. Schuitmaker, J. J., P. Bass, H. L. L. M. Van Leengoed, F. W. Van Der Meulen, W. M. Star and N. Zandwijk (1996) Photodynamic therapy: A promising new modality for the treatment of cancer. J.Photochem. Photobiol., B 34, 3–12.

9. Castano, A. P., T. N. Demidova and M. R. Hamblin (2005) Mechanisms in photodynamic therapy: part two—cellular signaling, cell metabolism and modes of cell death. Photodiag. Photodyn. Ther. 2, 1–23.

10. Krasnovsky Jr. A. A., (2007) Primary mechanisms of photoactivation of molecular oxygen. History of development and the modern status of research, Biochemistry (Moscow), 72, 1065–1080.

11. MacDonald, I. J. and T. J. Dougherty (2001) Basic principles of photodynamic therapy.

J. Porphyrins Phthalocyanines 5, 105–129.

12. Dolmans, D. E. J. G. J., D. Fukurama and R. K. Jain (2003) Photodynamic therapy for cancer. Nat. Rev. Cancer 3, 380–387.

13. Detty, M. R., S. L. Gibson and S. J. Wagner (2004) Current clinical and preclinical photosensitizers for use in photodynamic therapy. J.Med. Chem. 47, 3897–3915.

14. Weissleder, R. (2001) A clearer vision for in vivo imaging. Nat. Biotechnol. 19, 316–317.

15. Ochsner, M. (1996) Light scattering of human skin: A comparison between zinc(II)—phthalocyanine and photofrin IIㅜ. J. Photochem. Photobiol., B 32, 3–9.

16. Eichler, J., J. Knof and H. Lenz (1977) Measurements on the depth of penetration of light (0.35–1.0 lm) in tissue. Radiat. Environ. Biophys. 14, 239–242.

17. Wilson, B. C., W. P. Jeeves, D. M. Lowe and G. Adam (1984) Light propagation in animal tissues in the wavelength range 375-825 nanometers. Progr. Clin. Biol. Res. 170, 115–132.

18. Yakubovskaya, R. I., V. K. Oganezov, L. A. Shytova, T. A. Karmakova, G. N. Vorozhtsov and S. G. Kuzmin (1996) Photodynamic activity of a number of photosensitizers in vitro. Proc. SPIE – Inter. Soc. Optic. Eng. 2924, 75–85.

19. Lin, C.-W., J. R. Shulok, Y. K. Wong, L. Cincotta and J. W. Foley (1990) Uptake, retention, and phototoxicity of cationic phenoxazines photosensitizers in tumor cells in culture. Proc. SPIE - Inter. Soc. Optic. Eng. 1203, 287–292.

20. Luo, S., E. Zhang, Y. Su, T. Cheng and C. Shi (2011) A review of NIR dyes in cancer targeting and imaging. Biomaterials 32, 7127–7138.

21. Escobedo, J. O., O. Rusin, S. Lim and R. M. Strongin (2010) NIR dyes for bioimaging applications. Curr. Opin. Chem. Biol. 14, 64–70.

22. Lee, C., S. S. Wu and L. B. Chen (1995) Photosensitization by 3,3′ -dihexyloxacarbocyanine iodide: Specific disruption of microtubules and inactivation of organelle motility. Cancer Res. 55, 2063–2069.

23. Ara, G., J. R. Aprille, C. D. Malis, S. B. Kane, L. Cincotta, J. Foley, J. V. Bonventre and A. R. Oseroff (1987) Mechanisms of mitochondrial photosensitization by the cationic dye, N, N′-Bis(2-ethyl-l,3-dioxylene)kryptocyanine (EDKC): Preferential inactivation of complex I in the electron transport chain. Cancer Res. 47, 6580–6585.

24. Oseroff, A. R., D. Ohuoha, G. Ara, D. Mcauliffe, J. Foley and L. Cincotta (1986) Intramitochondrial dyes allow selective in vitro photolysis of carcinoma cells. Proc. Natl Acad. Sci. USA 83, 9729–9733.

25. Devi, D. G., T. R. Cibin, D. Ramaiah and A. Abraham (2008) Bis(3,5-diiodo-2,4,6-trihydroxyphenyl)squaraine: A novel candidate in photodynamic therapy for skin cancer models in vivo. J. Photochem. Photobiol., B 92, 153–159.

26. Ramaiah, D., I. Eckert, K. T. Arun, L. Weidenfeller and B. Epe (2002) Squaraine dyes for photodynamic therapy: Study of their cytotoxicity and genotoxicity in bacteria and mammalian cells. Photochem. Photobiol. 76, 672–677.

27. Ramaiah, D., A. Joy, N. Chandrasekhar, N. V. Eldho, S. Das and M. V. George (1997) Halogenated squaraine dyes as potential photochemotherapeutic synthesis and study of photophysical properties and quantum efficiencies of singlet oxygen generation. Photochem. Photobiol. 65, 785–790.

28. Ramaiah, D., I. Eckert, K. T. Arun, L. Weidenfeller and B. Epe (2004) Squaraine dyes for photodynamic therapy: Mechanism of cytotoxicity and DNA damage induced by halogenated squaraine dyes plus light (>600 nm). Photochem. Photobiol. 79, 99–104.

29. Beverina, L., A. Abbotto, M. Landenna, M. Cerminara, R. Tubino, F. Meinardi, S. Bradamante and G. A. Pagani (2005) New p-extended water-soluble squaraines as singlet oxygen generators. Org. Lett. 7, 4257–4260.

30. Santos, P. F., L. V. Reis, I. Duarte, J. P. Serrano, P. Almeida, A. S. Oliveira and L. F. V. Ferreira (2005) Synthesis and photochemical evaluation of iodinated squarylium cyanine dyes. Helv. Chim. Acta 88, 1135–1143.

31. Beverina, L., M. Crippa, M. Landenna, R. Ruffo, P. Salice, F. Silvestri, S. Versari, A. Villa, L. Ciaffoni, E. Collini, C. Ferrante, S. Bradamante, C. M. Mari, R. Bozio and G. A.

Pagani (2008) Assessment of water-soluble p-extended squaraines as one- and two-photon singlet oxygen photosensitizers: Design, synthesis, and characterization. J. Am. Chem. Soc. 130, 1894–1902.

32. Luo, C., Q. Zhou, G. Jiang, L. He, B. Zhang and X. Wang (2011) The synthesis and $^1O_2$ photosensitization of halogenated asymmetricaniline-based squaraines. New J. Chem. 35, 1128–1132.

33. Arunkumar, E., P. K. Sudeep, P. V. Kamat, B. C. Nolla and B. D.Smith (2007) Singlet oxygen generation using iodinated squaraine and squaraine - rotaxane dyes. New J. Chem. 31, 677–683.

34. Rapozzi, V., L. Beverina, P. Salice, G. A. Pagani, M. Camerin and L. E. Xodo (2010) Photooxidation and phototoxicity of p-extended squaraines. J. Med. Chem. 53, 2188–2196.

35. Avirah, R. R., D. T. Jayaram, N. Adarsh and D. Ramaiah (2012) Squaraine dyes in PDT: From basic design to in vivo demonstration. Org. Biomol. Chem. 10, 911–920.

36. Yogo, T., Y. Urano, Y. Ishitsuka, F. Maniwa and T. Nagano (2005) Highly efficient and photostable photosensitizer based on BODIPY chromophore. J. Am. Chem. Soc. 127, 12162–12163.

37. Lim, S. H., C. Thivierge, P. Nowak-Sliwinska, J. Han, H. van den Bergh, G. Wagnieres, K. Burgess and H. B. Lee (2010) In vitro and in vivo photocytotoxicity of boron dipyrromethene derivatives for photodynamic therapy. J. Med. Chem. 53, 2865–2874.

38. Ozlem, S. and E. U. Akkaya (2009) Thinking outside the silicon box: Molecular and logic as an additional layer of selectivity in singlet oxygen generation for photodynamic therapy. J. Am. Chem. Soc. 131, 48–49.

39. Awuah, S. G., J. Polreis, V. Biradar and Y. You (2011) Singlet oxygen generation by novel NIR BODIPY dyes. Org. Lett. 13, 3884–3887.

40. Killoran, J., L. Allen, J. F. Gallagher, W. M. Gallagherb and D. F. O'Shea, (2002) Synthesis of BF2 chelates of tetraarylazadipyrromethenes and evidence for their photodynamic therapeutic behavior. Chem. Commun. 1862–1863.

41. Byrne, A. T., A. E. O'Connor, M. Hall, J. Murtagh, K. O'Neill, K. M. Curran, K.

Mongrain, J. A. Rousseau, R. Lecomte, S. McGee, J. J. Callanan, D. F. O'Shea and W. M. Gallagher (2009) Vascular-targeted photodynamic therapy with BF2-chelated tetraaryl-azadipyrromethene agents: A multi-modality molecular imaging approach to therapeutic assessment. Br. J. Cancer 101, 1565–1573.

42. Adarsh, N., R. R. Avirah and D. Ramaiah (2010) Tuning photosensitized singlet oxygen generation efficiency of novel aza-BODIPY dyes. Org. Lett. 12, 5720–5723.

43. Das, S., K. G. Thomas and M. V. George, (1997) Photophysical and Photochemical Properties of Squaraines in Homogeneous and Hetergeneous Media. In Organic Photochemistry, (Edited by V. Ramamuthy and K. S. Schanze), pp. 67–517. Marcel Decker, Inc, New York.

44. Beverina, L. and P. Salice (2010) Squaraine compounds: Tailored design and synthesis towards a variety of material science applications. Eur. J. Org. Chem., 1207–1225.

45. Ajayaghosh, A. (2005) Chemistry of squaraine-derived materials: Near-IR dyes, low band gap systems, and cation sensors. Acc. Chem. Res. 38, 449–459.

46. Berlman, I. B. (1973) Empirical study of heavy-atom collisional quenching of the fluorescence state of aromatic compounds in solution. J. Phys. Chem. 77, 562–567.

47. Wilcox, W. S., D. P. Grisswoldd, W. R. Laster, F. M. J. Schabel and H. E. Skipper (1965) Experimental evaluation of potenital anticancer agents. XVII. Kinetics of growth and regression after treatment of certain solid tumors. Cancer Chemother Res. 47, 27–39.

48. Strober, W., Trypan blue exclusion test of cell viability Curr. Protoc.Immunol. A.3.B.1 –A.3.B.2

49. Bilmes, G. M., J. O. Tocho and S. E. Braslavsky (1989) Photophysical processes of polymethine dyes. An absorption, emission, and optoacoustic study on 3,3′ -diethylthiadicarbocyanine iodide. J. Phys. Chem. 93, 6696–6699.

50. Yarborough, J. M. (1974) CW dye laser emission spanning the visible spectrum. Appl. Phys. Lett. 24(12), 629–630.

51. Gollnick, K. and A. Griesbeck (1985) Singlet oxygen photooxygenation of furans: Isolation and reactions of (4+2)-cycloaddition products (unsaturated sec.-ozonides).

Tetrahedron 41, 2057–2068.

52. Wang, H. and J. A. Joseph (1999) Quantifying cellular oxidative stress by dichlorofluorescein assay using microplate reader. Free Radical Biol. Med. 27, 612–616.

53. Hussain, S. M., K. L. Hess, J. M. Gearhart, K. T. Geiss and J. J. Schlager (2005) In vitro toxicity of nanoparticles in BRL 3A rat liver cells. Toxicol. In Vitro 19, 975–983.

54. Thomas, J., D. B. Sherman, T. J. Amiss, S. A. Andaluz and J. B. Pitner (2007) Synthesis and biosensor performance of a near-IR thiol-reactive fluorophore based on benzothiazolium squaraine. Bioconjugate Chem. 18, 1841–1846.

55. Tatarets, A. L., I. A. Fedyunyaeva, E. A. Terpetschnig and L. D. Patsenker (2005) Synthesis of novel squaraine dyes and their intermediates. Dyes Pigm. 64, 125–134.

56. Benz, M., A. M. van der Kraan and R. Prins (1998) Reduction of aromatic nitrocompounds with hydrazine hydrate in the presence of an iron oxide hydroxide catalyst II activity, X-ray diffraction and MoEssbauer study of the iron oxide hydroxide catalyst. Appl. Cat. A. 172, 149–157.

57. Bigelow, R. W. and H. J. Freund (1986) An MNDO and CNDO / S (S + DES CI) study on the structural and electronic properties of a model squaraine dye and related cyanine. Chem. Phys. 107, 159–174.

58. Cramer, L. E. and K. G. Spears (1978) Hydrogen bond strengths from solvent-dependent lifetimes of rose bengal dye. J. Am. Chem. Soc. 100, 221–227.

59. Moog, R. S., N. A. Burozski, M. M. Desai, W. R. Good, C. D. Silvers, P. A. Thompson and J. D. Simon (1991) Solution photophysics of 1- and 3-aminofiuorenone: The role of inter- and intramolecular hydrogen bonding in radilationless deactivation. J. Phys. Chem. 95, 8466–8473.

60. Das, S., K. G. Thomas, R. Ramanathan, M. V. George and P. V. Kamat (1993) Photochemistry of squaraine dyes. 6. Solvent hydrogen bonding effects on the photophysical properties of bis(benzothiazoly1idene)squaraines. J. Phys. Chem. 97, 13625–13628.

61. Das, S., K. G. Thomas, K. J. Thomas, P. V. Kamat, M. V. George and S. Das (1994) Photochemistry of squaraine dyes. 8. Photophysical properties of crown ether squaraine

fluoroionophores and their metal ion complexes. J. Phys. Chem. 98, 9291–9296.

62. Das, S., T. L. Thanulingam, K. G. Thomas, P. V. Kamat and M. V. George (1993) Photochemistry of squaraine dyes. 5. Aggregation of bis (2,4-dihydroxyphenyl)squaraine and Bis(2,4,6-trihydroxyphenyl) squaraine and their photodissociation in acetonitrile solutions. J. Phys. Chem. 97, 13620–13624.

63. Das, S., K. G. Thomas, K. J. Thomas, V. Madhavan, D. Liu, P. V. Kamat and M. V. George (1996) Aggregation behavior of water soluble bis(benzothiazolylidene) squaraine derivatives in aqueous media. J. Phys. Chem. 100, 17310–17315.

64. Santhosh, U. and S. Das (2000) Triplet excited-state properties of the monomer and aggregate of bis(2,4,6-trihydroxyphenyl)squaraine. J. Phys. Chem. A 104, 1842–1847.

65. Alex, S., M. C. Basheer, K. T. Arun, D. Ramaiah and S. Das (2007) Aggregation properties of heavy atom substituted squaraine dyes: Evidence for the formation of J-type dimer aggregates in aprotic solvents. J. Phys. Chem. A 111, 3226–3230.

66. Mayerh€offer, U., B. Fimmel and F. W€urthner (2011) Bright nearinfrared fluorophores based on squaraines by unexpected halogen effects. Angew. Chem. Int. Ed. 51, 164–167.

67. Patrick, B., M. V. George, P. V. Kamat, S. Das and K. G. Thomas (1992) Photochemistry of squaraine dyes: Excited states and reduced and oxidized forms of 4-(4-Acetyl-3,5-dimethylpyrrolium-2-ylidene)-2-(4- acetyl-3,5-d imethylpyrrol-2-yl)-3-oxocyclobut-1 –en4 -olate. J. Chem. Soc., Faraday Trans. 88, 671–676.

68. Kamat, P. V., S. Das, K. G. Thomas and M. V. George (1992) Photochemistry of squaraine dyes. 1. Excited singlet, triplet, and redox states of bis[4-(dimethylamino)phenyl]squaraine and bis[4-(dimethylamino)-2-hydroxyphenyl] squaraine. J. Phys. Chem. 96, 195–199.

69. Sauve, G., P. V. Kamat, K. G. Thomas, K. J. Thomas, S. Das and M. V. George (1996) Photochemistry of squaraine dyes: Excited triplet state and redox properties of crown ether squaraines. J. Phys. Chem. 100, 2117–2124.

70. Thomas, K. G., K. J. Thomas, S. Das, M. V. George, D. Lid and P. V. Kamat (1996) Photochemistry of squaraine dyes Part l0".Excitedstate properties and photosensitization

behaviour of an IR sensitive cationic squaraine dye. J. Chem. Soc., Faraday Trans. 92, 4913–4916.